

**NUMERICAL SIMULATION OF A CONTAMINATED DROPLET
BY FRONT-TRACKING METHOD
TAKING THE EFFECT OF SURFACTANT TRANSPORT ON THE INTERFACE**

Yasufumi Yamamoto
Department of Systems
Management Engineering,
Kansai University
3-3-35 Yamate-cho Suita
564-8680, Japan
yamayas@kansai-u.ac.jp

Makoto Yamauchi
Osaka Prefectural College
of Technology
26-12 Saiwai-cho Neyagawa,
Osaka, 572-8572, Japan
yamauchi@ipc.osaka-pct.ac.jp

Tomomasa Uemura
Department of Systems
Management Engineering,
Kansai University
umra@kansai-u.ac.jp

ABSTRACT

In this study, a front-tracking (FT) method combined with a solver of interfacial transport of surfactant was proposed in order to resolve interfacial flows affected by contamination. In the FT method, because the interfaces are presented explicitly, advection-diffusion equation on the interface can be easily treated and can be solved highly accurately. In this study, a scheme which conserves the total amount of surfactant completely was constructed. Numerical simulations of a water drop sinking in silicone oil were performed taking the Marangoni effect into account. The effects of three parameters, a damping coefficient of interfacial tension, a diffusion coefficient and a total amount of surfactant, were evaluated. Calculated results were compared with PTV measurement results and were in very good agreement with them on the points of stagnant cap size, flow separation point, peak of shear stress and so on. So, we can expect that our simulations can estimate the conditions of surfactant on the interfaces, which is very difficult to be measured.

INTRODUCTION

The effect of contamination of interfaces in gas-liquid or liquid-liquid two-phase flow systems have been studied in various way (for example, [1]), because the contamination does not only suppress the terminal velocity, but affects the transport of mass, momentum, and energy between phases. Yamauchi, Ozawa & Uemura[2] and Uemura & Yamauchi[3] developed the PTV technique that can simultaneously measure velocity fields on both sides of the interface of a water droplet sinking in oil, then evaluated the degree of contamination by the shearing condition on both sides of the interface. There are

some numerical studies of the contamination, which are based on boundary fitted coordinates (BFC) calculations[4-8]. In their calculations, the inner flow of gas bubble was neglected. However, when our interesting subject is liquid-liquid system, the inner flow of liquid drop cannot be negligible. It is because the densities of both phases are in the same order.

Recently, some methods to solve multi-phase flow problems using fixed rectangular grids, as VOF[9], Front-tracking[10], level-set[11], CIP[12], and so on, have been developed and are being widely used. James & Lowengrub[13] incorporated a model of surfactant transport on the interface into VOF and evaluated the effect of surfactant on the drop deformation. And Xu & Zhang[14] developed an Eulerian formulation of surfactant transport on the moving interface in the framework of level-set method. In VOF and level-set, however, interfaces are presented implicitly, so there are many difficulties in calculation of advection or derivative on the interface. On the other hand, in Front-tracking (FT), interfaces are explicitly presented, so advection and tangential derivative can be calculated easily and accurately. And, the effect of interfacial tension is given directly as the difference of tangential tension, so the Marangoni effect can be easily presented. Jan & Tryggvason[15] performed FT simulations taking the interfacial advection of surfactant into account to examine the change of bubble rising velocity. In their model, diffusion and adsorption/desorption process were neglected. Homma, Koga, Matsumoto & Tryggvason [16] combined transport of solute in the bulk phase into FT simulations. Calculation of the bulk concentration of solute was not directly incorporated with merits of the FT.

In this study, we propose the simulation method using FT method combined with a solver of the transport of surfactant on the interface. At first, a fully conservative scheme of the advection-diffusion solver on the interface is presented, which uses the characteristic of the FT method skillfully. The effect of parameters of the surfactant transport is examined. Then, we try to reproduce the experimental results of contaminated droplet measured by Yamauchi et al.[2,3]. If a set of parameters at which the simulation reproduces the experimentally observed result was found, we can estimate the real surfactant conditions by them.

In the present state of this study, however, we neglect the adsorption/desorption process, in order to simplify the model and to reduce the number of parameters.

NOMENCLATURE

d_d	Droplet diameter
D_s	Interfacial diffusion coefficient
\mathbf{g}	Gravity acceleration vector
l	Length of front segment
\mathbf{n}	Unit vector normal to the interface
p	Pressure
r	Radial coordinate
Re	Reynolds number ($=d_d U_d / \nu$)
s	Length coordinate tangent to the interface
Sc_s	Schmidt number ($=\nu/D_s$)
\mathbf{t}	Unit vector tangent to the interface
\mathbf{u}	Velocity vector
U_d	Terminal velocity of the drop
x	Horizontal coordinate
z	Vertical coordinate
α	Damping coefficient of interfacial tension
ϕ	Circumferential coordinate
Γ	Non-dimensional concentration on the interface
μ	Viscosity
ν	Kinematic viscosity
θ	Azimuthal coordinate
ρ	Density
σ	Interfacial tension

TARGET OF SIMULATION

As the target of simulations in this study, a water drop sinking in a silicone oil, which was measured in detail by Yamauchi et al.[3], was chosen. 100cSt silicone oil (temperature 25 °C, $\rho = 965.0 \text{ kg/m}^3$, $\mu = 9.65 \times 10^{-2} \text{ Pa s}$, $\sigma_{oil} = 2.09 \times 10^{-2} \text{ N/m}$) is filled in the 31mm diameter-cylindrical tube. In the tube, a water drop (temperature 25 °C, $\rho_{water} = 997.1 \text{ kg/m}^3$, $\mu_{water} = 8.904 \times 10^{-4} \text{ Pa s}$, $\sigma_{water} = 7.196 \times 10^{-2} \text{ N/m}$) sinks by the gravitational force. And the droplet diameter is set to $d_d = 15.4 \text{ mm}$ (Reynolds number of the experimental result $Re = \rho d_d U_d / \mu$ is 2.7). The flow field is axisymmetric because the ratio of the droplet diameter to the tube diameter is not so large. Then, our simulations were performed on the axisymmetric cylindrical coordinates. The calculated results are presented on

the polar coordinates (r, θ, ϕ) , whose origin is at the center of the droplet. In order to avoid confusion, the cylindrical coordinates are represented by (x, ϕ, z) .

We do not have any information about the surfactant (e.g. physical properties, concentration) contained in the experimental apparatus. Then, we do not know whether the adsorption/desorption process can be neglected or not. Anyway we try to perform simulations without adsorption/desorption process as the first challenge of this study. We analyze results at a fully developed state. Three parameters of the initial uniform concentration Γ_0 , the diffusion coefficient on the interface D_s (corresponding to non-dimensional parameter of Schmidt number $Sc_s = \nu/D_s$, where ν is kinematic viscosity of oil) and the damping coefficient α of interfacial tension (described later) are adjusted to reproduce the flow field observed in the experiment. From the calculated results, surfactant conditions are estimated.

NUMERICAL PROCEDURE

Summary of Front-tracking method

In this section, we briefly describe an overview of the FT method (more detail is described in reference [17]).

One of most characteristic features of the FT is that the interfaces are represented explicitly by connected marker points as front points. The front points are moved with a velocity interpolated from velocities at fixed grid points. A Heaviside function, which smoothly varies at the interface, is defined on each fixed grid points, by using the front points' locations and normal vectors. Densities and viscosities on the grid points are given by the linear function of the Heaviside function. The interfacial tension force acting on each front element (line segment) can be calculated accurately by using tangent vectors at front points. Conversion of information between front elements and fixed grid points are done through a weight function with width of ± 2 grid interval. In FT, basic equations are solved on the fixed grid system, with assistance of Lagrangean front points. FT is the method that treats the multi-fluid system as one fluid, whose density and viscosity varies spatially, and in which interfacial tension force acts as the delta function body force.

In this study, fluids are assumed to be incompressible. Basic equations are following two equations.

$$\rho \left\{ \frac{\partial \mathbf{u}}{\partial t} + \nabla \cdot \mathbf{u} (\mathbf{u} - \mathbf{u}_g) \right\} \quad (1)$$

$$= -\nabla p + \nabla \cdot \mu (\nabla \mathbf{u} + \nabla \mathbf{u}^T) + \mathbf{F}_s + \rho \mathbf{g} \quad (2)$$

$$\nabla \cdot \mathbf{u} = 0$$

In order to get a fully developed state on a high resolution grid system, the grid points are moved with the same velocity of the tip of the drop \mathbf{u}_g . So, advection velocity in equation (1) is presented as the relative velocity. \mathbf{F}_s is the interfacial tension force converged to body force exerting only the volume near

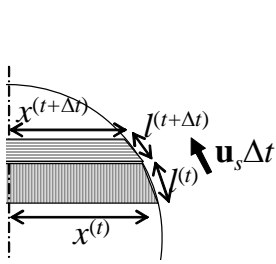


Fig.1 Advection of surfactant and area on the interface.

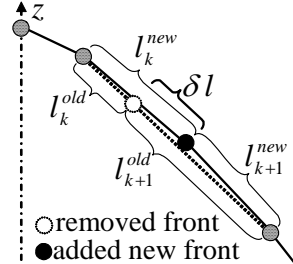


Fig.2 Redistribution of front points

the interface. These equations are discretized in space by a second order central finite difference. A second-order Adams-Bashforth method is applied for time marching of advection term, and a second-order Crank-Nicolson scheme is applied for viscous term. Other terms are treated by a first-order implicit scheme.

Transport of surfactant

For the surfactant concentration on the interface Γ , the advection-diffusion equation is considered, neglecting adsorption/desorption. The basic equation is derived by Stone[18],

$$\frac{\partial \Gamma}{\partial t} + \nabla_s \cdot (\mathbf{u}\Gamma) = D_s \nabla_s^2 \Gamma \quad (3)$$

where ∇_s is the surface gradient. In our calculation, left hand side term representing advection is not approximated by finite difference. But advection is represented by Lagrangean movement of the front elements. The amount of substance not concentration is stored on the center of each front element, so that surfactant advection is automatically represented by the movement of each front element. A change of the concentration due to the change of the interface area is also automatically represented by the change of front element's length, which is automatically changed by the movement of individual front points. For example in the case shown in Fig. 1, update of the concentration is given by the following.

$$2\pi x^{(t+\Delta t)} l^{(t+\Delta t)} \Gamma^{(t+\Delta t)} = 2\pi x^{(t)} l^{(t)} \Gamma^{(t)} \quad (4)$$

As front points move individually, the elements may become extremely coarse or crowded. In order to avoid the difference of resolution, appropriate addition and deletion of front points are needed. We propose a scheme paying attention to the requirement which the total amount of surfactant is conserved during this process. For example, Fig. 2 shows front elements (l_k^{old} corresponding to $l^{(t+\Delta t)}$ in Fig. 1) before and after a deletion and an addition. At first, the point \circ is deleted because the length of the element l_k^{old} is shorter than a threshold. Then, the new length of the element $l_k^{old} + l_{k+1}^{old}$ becomes longer than a threshold. Subsequently, the new point \bullet is added (for more

detail about addition, see reference [17]). Surfactant is redistributed so that the amount of substances contained in the elements with the same area conserves. Namely, in Fig. 2, an attention is paid to the region δl , which changes the belonging element. The amount of surfactant contained in the new element l_k is given by the following,

$$2\pi x_k^{new} l_k^{new} \Gamma_k^{new} = 2\pi x_k^{old} l_k^{old} \Gamma_k^{old} + 2\pi X \delta l \Gamma_{k+1}^{old} \quad (5)$$

where x -coordinate of the center of the element δl is X , that of l_k^{new} is x_k^{new} , and so on. The amount of surfactant in the element l_{k+1} is decreased in the same amount of the increase in equation (5). By this proposed series of advection calculation, the total amount of surfactant conserves completely.

The diffusion term of surfactant transport is treated by a fractional step method. The concentration after the advection (presented by superscript $*$) is discretized on the front element spatially by a central finite difference,

$$\frac{\Gamma^{(n+1)} - \Gamma^*}{\Delta t} = D_s \frac{1}{x} \frac{\partial}{\partial s} \left(x \frac{\partial \Gamma}{\partial s} \right) \quad (6)$$

where s is length coordinate tangent to the interface. For time marching of advection (corresponding to front displacement), a second-order Adams-Bashforth method is applied, and a second-order Crank-Nicolson scheme is applied for diffusion term.

Relation of interfacial tension on the interface concentration of surfactant is given by Langmuir model,

$$\sigma = \sigma_0 \{1 + \alpha \ln(1 - \Gamma)\} \quad (7)$$

where σ_0 is interfacial tension ($\sigma_{water} - \sigma_{oil}$) for a clean interface. The interface concentration is non-dimensionalized by the maximum interface concentration Γ_∞ . The damping coefficient α is represented by the ratio of Marangoni number $Ma = R_G T \Gamma_\infty / (\mu U_d)$ to capillary number $Ca = \sigma_0 / (\mu U_d)$, $\alpha = Ma / Ca$, where R_G is the gas constant, T is absolute temperature.

In our simulation, drops are freely falling, so terminal velocity U_d cannot be given as a preset condition. Then, we set α as one of the preset conditions. In the case of neglecting desorption, surfactant may be unlimitedly accumulated, then the maximum interface concentration cannot be defined. If non-dimensional concentration exceeds 1, equation (7) cannot be evaluated. However, within the range of our simulation conditions, because the Marangoni effect suppresses advection through equation (7), the non-dimensional concentration did not exceed 1.

The interfacial tension force exerted on a front element in FT, is given by the difference of tangential tension and the effect of curvature in the circumferential direction,

$$\mathbf{f}(\mathbf{x}_s)\Delta s = (\sigma\mathbf{t})^+ - (\sigma\mathbf{t})^- + \sigma^{mid} \frac{n_x}{x} \mathbf{n}\Delta s \quad (8)$$

where superscripts +, -, and *mid* are both ends of the front element and the center, respectively, Δs is length of the element, \mathbf{n} is the unit normal vector, \mathbf{t} is the unit tangent vector. By equation (8), the interfacial tension force can be accurately presented and the spatial change of σ is easily represented. \mathbf{F}_s in equation (1) is given by distributing $\mathbf{f}(\mathbf{x}_s)\Delta s$ onto fixed grid points through the weight function.

RESULT

Simulation condition

All the calculations begin from a condition at which both phase are stationary, then the flow field is developed by a freely falling drop. All the results shown in this paper are the ones at fully developed state. $\theta=0$ on the polar coordinates indicates the bottom of the drop.

At first, the effect of spatial resolution of the fixed grid system was evaluated. Figure 3 shows the velocity distribution of vertical component on the horizontal line through the droplet center. Because the simulated drop's shape is approximately spherical, 1 on the horizontal axis corresponds to the interface position. Three conditions of spatial resolution (A: the number of grid points 31×124 , $\Delta x/d_d=0.032$, B: 62×248 , $\Delta x/d_d=0.016$, C: 124×496 , $\Delta x/d_d=0.008$) are tested using appropriate parameters discussed in detail later ($\Gamma_0=0.15$, $\alpha=0.015$, $Sc_s=40$). At the interface, the salient point is shifted into the low viscosity fluid within the width of the weight function as mentioned in reference [19], so the substantial interface position in the low resolution case (A) differs largely from the experimental measurement. The result in case (B) shows somewhat difference from the experimental one, but higher resolution calculation (C) does not show effective improvement. In the same figure, result in the other concentration case $\Gamma_0=0.45$ on the B grid system is also shown.

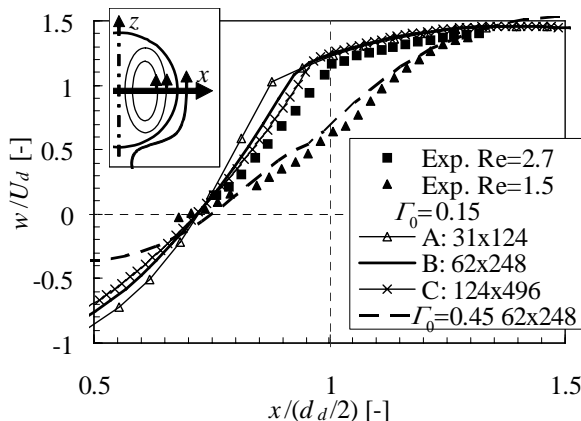


Fig.3 Distribution of vertical velocity component on the horizontal line through the droplet center.

Comparison of this calculated result with more contaminated experimental result ($Re=1.5$) show very good agreement. Then, in this study, grid system (B) is used for all simulations presented hereafter. The time increment is decided as $\Delta t = 2.5 \times 10^{-4}$ s by trial and error.

For evaluation of velocity gradient at the interface inside the drop, taking the salient point into account, the gradient is calculated by a one-side finite difference at the point 2-grid size apart from the interface. On the other hand, the experimentally measured data are redistributed on the grid system with $\Delta x/d_d = 0.013$, then gradient is obtained by the analytical derivative of a fitted curve of velocity profile.

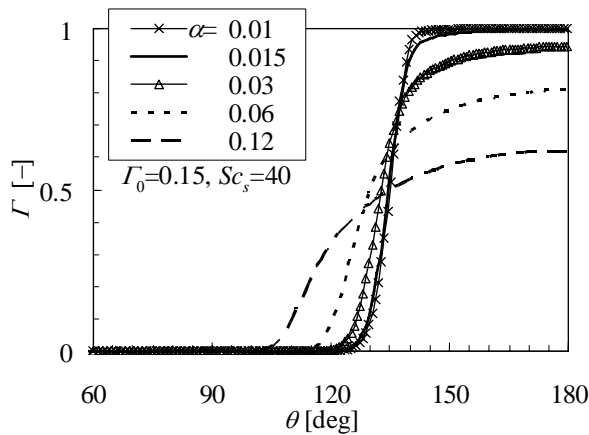
Effect of damping coefficient of interfacial tension

Figure 4 shows the effect of the damping coefficient α on (a) concentration profile, (b) tangential velocity profile, and (c)(d) radial gradient of tangential velocity outside and inside the drop. From Fig. 4(a), we can find out that α changes the region existing the surfactant. Each corresponding points in (a)-(d) are noticed as following. The tangential velocity changes largely at the position which the concentration begins to increase. Both of the outside and the inside velocity gradients have each peak at the position which the interface velocity drops to zero. Increase of α makes those positions (concentration increasing point, velocity decreasing point, and peak point of velocity gradient) moved forwards.

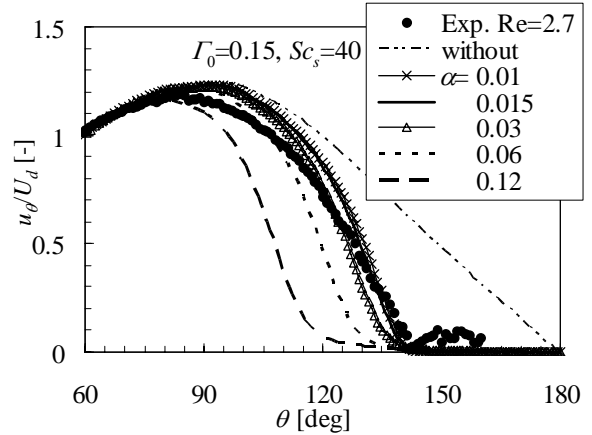
Effect of diffusion coefficient

Figure 5 shows the effect of Schmidt number Sc_s on the same kinds of quantities as those in Fig. 4. In this paper, variation of Sc_s corresponds simply to variation of the interfacial diffusion coefficient D_s because of constant viscosity. In the case of high Sc_s , advection transports surfactant one-sidedly to backward, then, the rear part of the drop has the large concentration. At the same time, the boundary of high concentration region becomes sharp. As a main tendency of the concentration profile, Sc_s does not change the inflection point but changes the tangential gradient of profile.

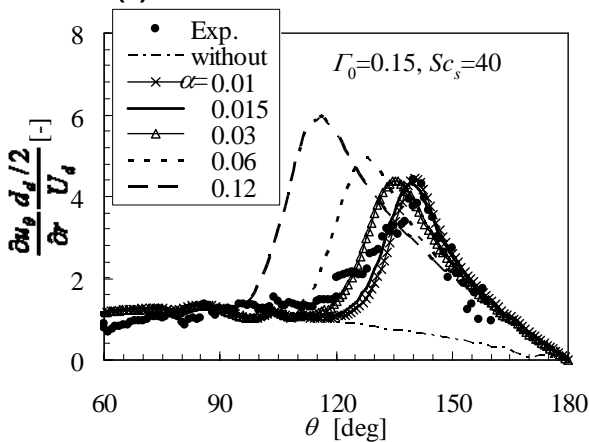
As shown in the Fig. 4 for the effect of α , velocity changes largely at the point where the concentration starts to increase. On the other hand, in the case of small α , even though large diffusion makes the concentration's increasing point move forward, velocity profile changes little because of small gradient of interfacial tension. As the result shown in Figs. 5(a) and (b), velocity changes largely at the point where the concentration has steep gradient (around $\theta=130$). As increasing Sc_s , the region in which the concentration changes becomes narrow, then velocity changes sharply within that region. Following those changes, spatial gradients of velocity becomes large, then, radial gradients (Figs. 5(c) and (d)) also show intense peak around the region as increasing Sc_s .



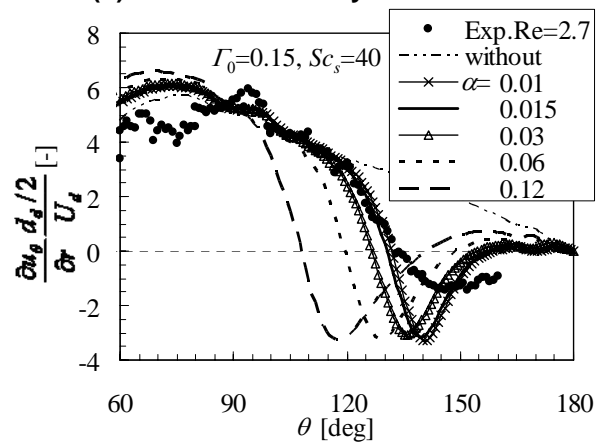
(a) concentration distribution



(b) interfacial velocity distribution



(c) radial gradient of tangential velocity outside of the interface



(d) radial gradient of tangential velocity inside of the interface

Fig.4 Effect of damping coefficient of interfacial tension α

Effect of total amount of surfactant

Figure 6 shows the effect of mean concentration Γ_0 , which corresponds to the total amount of adsorbed surfactant. In our simulation conditions of low diffusion coefficient, concentration at the rear part becomes nearly maximum value. So, the effect of Γ_0 appears the difference of concentration's increasing points (Fig. 6(a)). A change of tangential gradient of the concentration causes a change of velocity's decreasing points (Fig. 6(b)). Because velocity profile outside the drop has large difference in each θ position, radial velocity gradient changes not only the peak position but the peak value (Fig. 6(c)).

The condition at which a calculated result agrees with experimental one of $Re=2.7$ is the case of $\Gamma_0=0.15$, $\alpha=0.015$, $Sc_s=40$. Interfacial velocity at this condition shown in Fig.6(b) shows good agreement of edge location of stagnant cap, while peak velocity shows a little difference. Then, the peak location of radial velocity gradient and peak value outside the drop, agree very well with experimental one respectively, except for

the peak of inside gradient. Concerning the gradient inside the drop, the experimental measurement does not have high reliability due to low tracer concentration at the separation point, and one-fluid model simulation has the defect of velocity shift into low viscosity as mentioned before. Thereby, we compare only the rough tendency for the inside gradient. Furthermore, comparisons of calculated streamlines with experimental path lines are shown in Fig. 7. Reynolds numbers based on the terminal velocity are also shown in each caption. In the case of $\Gamma_0=0.15$, the similar features of simulated results, the dead water region in the drop rear, flow separation of outside wake, inner circulation, and so on, as those in the experimental observation of $Re=2.7$ are reproduced.

If the properties of surfactants are same through a series of experiments, we can guess that the difference of experimentally observed flow field of $Re=1.5$ on the same experimental facility is just caused by the difference of the total amount of surfactant. Compare calculated result of $\Gamma_0=0.45$ with fixed α and Sc_s with experimental results of $Re=1.5$, then flow field and terminal velocity shown in Figs. 7(d) and (e) show very

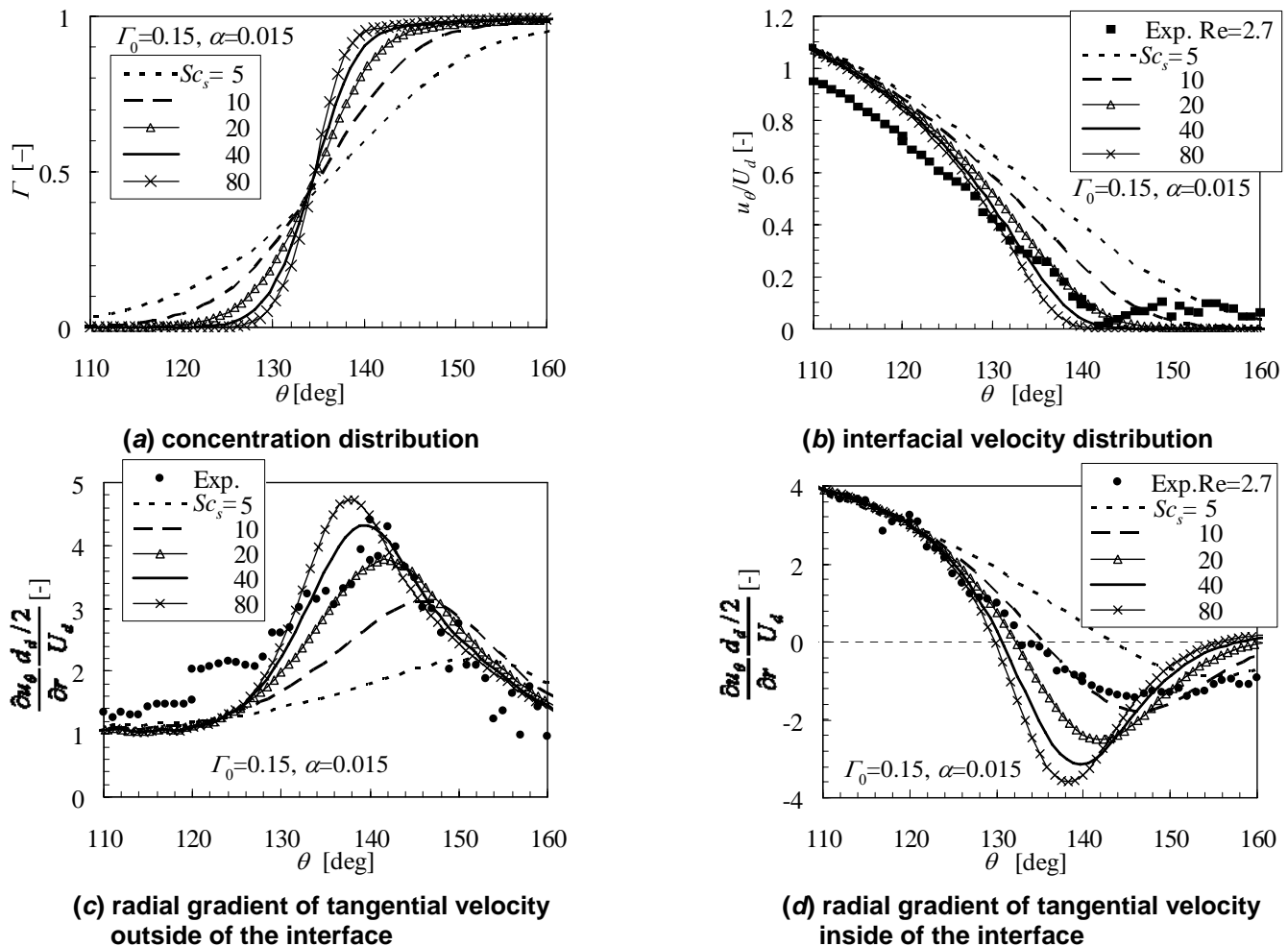


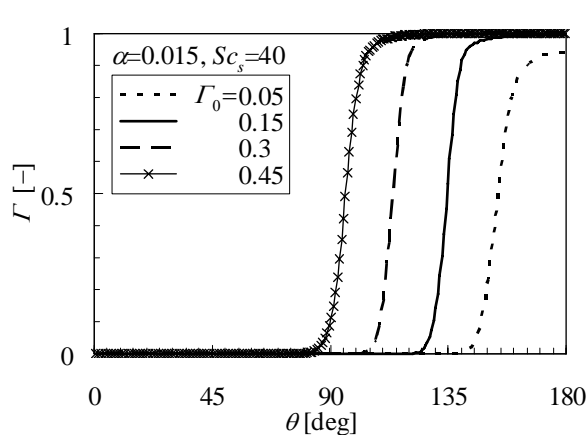
Fig.5 Effect of diffusion coefficient Sc_s .

good agreement. The interfacial velocity shown in Fig. 6(b) also shows good agreement except for the edge of the stagnant cap. At the edge of the stagnant cap (around $\theta=110$), flow separates and vary in high spatial frequency, however, measurement resolution is not enough high due to low tracer concentration. The calculated radial gradients shown in Figs. 6(c) and (d) show large peak at the separation point, while a portion of experimental results are scraped off around the separation point. These evidences assist the supposition of low measurement resolution. Except for the separation point, the radial gradient of the present simulation agree very well with the experimental results (Fig. 6(c) and (d)).

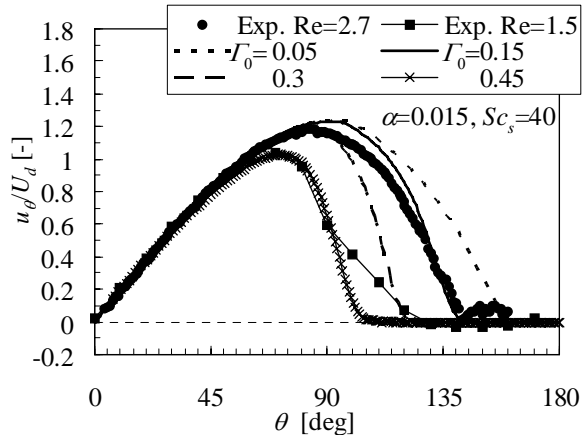
Summarizing the above results, we can consider the present simulation model reasonably represent the momentum balance of a falling drop at a fully-developed state, because calculated results show very good agreement with experimental measurements. However, the range of applicability is limited, because of neglecting the adsorption/desorption process. Discussion of the limit is the subject for a future study.

SUMMARY

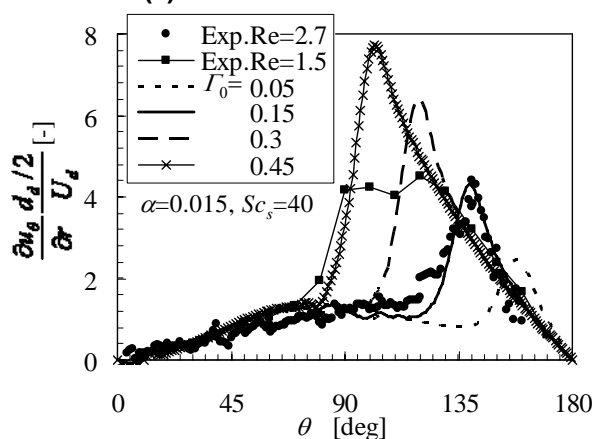
We proposed the Front-tracking method combined with a solver of surfactant transport on the interface. A concrete process of the advection-diffusion calculation on the explicitly represented interfaces was presented and a fully conservative scheme was proposed. Simulations of a water drop sinking in a silicone oil taking the Marangoni effect into account were performed. Three parameters of the damping coefficient of interfacial tension, the interfacial diffusion coefficient, and the total amount of surfactant, were evaluated and the tendencies of interface concentration, velocity, and velocity gradient were clarified. By the adjustment of those three parameters, the present simulation can reproduce experimentally observed drops accurately. In particular, the stagnant cap size, the location of separation point, the steep peak of velocity gradient and the terminal velocity were properly predicted. We can expect that our simulations can estimate the conditions of surfactant on the interfaces, which is very difficult to be measured.



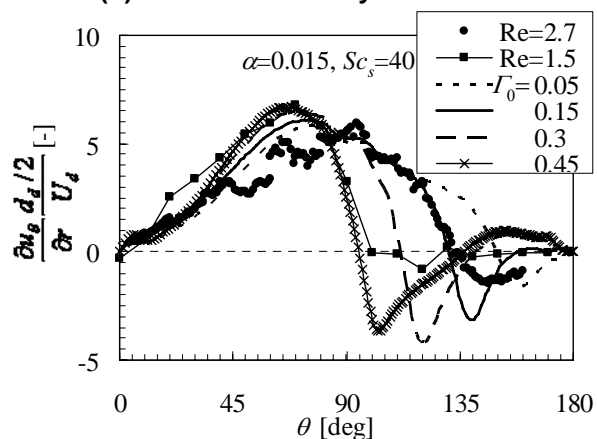
(a) concentration distribution



(b) interfacial velocity distribution



(c) radial gradient of tangential velocity outside of the interface



(d) radial gradient of tangential velocity inside of the interface

Fig.6 Effect of total mass of surfactant Γ_0 .

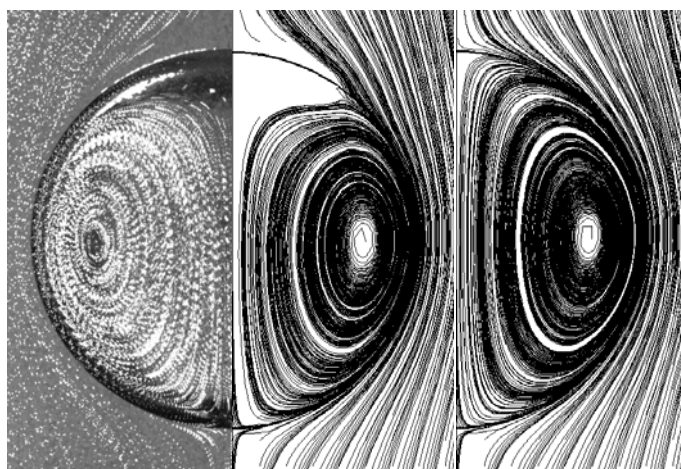
ACKNOWLEDGMENTS

This work is partially supported by the Japan Society for the Promotion of Science, Grant-in-Aid for Young Scientists (B) (17760149).

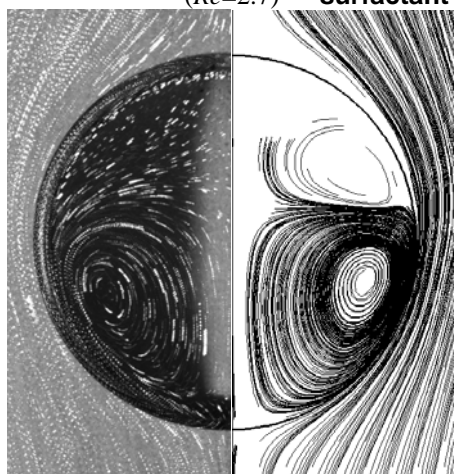
REFERENCES

- [1] Levich, V.G., 1962, *Physicochemical Hydrodynamics*, Prentice-Hall.
- [2] Yamauchi, M., Ozawa, M., and Uemura, T., 2000, "PTV Measurement at Close Region to Interface of a Water Drop in Oil", *Japanese Journal of Multiphase Flow*, **14**(4), pp. 466-472. (in Japanese)
- [3] Uemura T. and Yamauchi, M., 2001, "Shearing Conditions on the Interface of a Spherical Water Drop Sinking in Silicone Oil", *KSME International Journal*, **15**(12), pp. 1845-1852.
- [4] Bel Fdhila, R. and Duineveld, P.C., 1996, "The Effect of Surfactant on the Rise of a Spherical Bubble at High Reynolds and Peclet Numbers", *Physics of Fluids*, **8**(2), pp.310-321.

- [5] Cuenot, B., Magnaudet, J., and Spennato, B., 1997, "The Effects of Slightly Soluble Surfactants on the Flow around a Spherical Bubble", *Journal of Fluid Mechanics*, **339**, pp.25-53.
- [6] Takagi, S., Yamamoto, A., and Matsumoto, Y., 1999, "Numerical Analysis of a Rising Bubble in a Contaminated Liquid", *Proc. 3rd ASME/JSME Joint Fluids Engineering Conference*, FEDSM99-7102.
- [7] Liao, Y. and McLaughlin, J.B., 2000, "Bubble Motion in Aqueous Surfactant Solutions", *Journal of Colloid and Interface Science*, **224**, pp.297-310.
- [8] Takagi, S. and Matsumoto, Y., 2000, "Contaminant Effect on the Motion of a Rising Bubble", *Proc. ASME 2000 Fluids Engineering Division Summer Meeting*, FEDSM2000-11269.
- [9] Hirt, C.W. and Nichols, B.D., 1981, "Volume of Fluid (VOF) Method for the Dynamics of Free Boundaries", *Journal of Computational Physics*, **39**, pp.201-225.
- [10] Unverdi, S.O. and Tryggvason, G., 1992, "A Front-Tracking Method for Viscous, Incompressible, Multi-Fluid Flows", *Journal of Computational Physics*, **100**, pp.25-37.



(a) Exp. $Re=2.7$ (b) $\Gamma_0=0.15$ (c) without
 (Re=2.7) surfactant (Re=3.1)



(d) Exp. $Re=1.5$ (e) $\Gamma_0=0.45$ ($Re=1.6$)

Fig.7 Calculated streamlines ($\alpha=0.015$, $Sc_s=40$) and experimental path lines.

- [11] Sussman, M., Smereka, P., and Osher, S., 1994, "A Level Set Approach for Computing Solutions to Incompressible Two-Phase Flow", *Journal of Computational Physics*, **114**, pp.146-159.
- [12] Yabe, T., Xiao, F., and Utsumi, T., 2001, "The Constrained Interpolation Profile Method for Multiphase Analysis", *Journal of Computational Physics*, **169**, pp.556-593.
- [13] James, A.J. and Lowengrub, J., 2004, "Surfactant-Conserving Volume-of-Fluid Method for Interfacial Flows with Insoluble Surfactant", *Journal of Computational Physics*, **201**, pp. 685-722.
- [14] Xu, J.J. and Zhao, H.K., 2003, "An Eulerian Formulation for Solving Partial Differential Equations along a Moving Interface", *Journal of Scientific Computing*, **19**, pp.573-594.
- [15] Jan, Y. and Tryggvason, G., 1991, "Computational Studies of Contaminated Bubbles", *Proc. Dynamics of Bubbles and Vortices Near a Free surface, ASME/AMD* **119**, pp.59-64.
- [16] Homma, S., Koga, J., Matsumoto, S., and Tryggvason, G., 1999, "Solutal-Capillary Motion of a Liquid Jet and its Breakup into Drops", *Proc. 3rd ASME/JSME Joint Fluids Engineering Conference, FEDSM99-7114*.
- [17] Tryggvason, G., Bunner, B., Esmaeeli, A., Juric, D., Al-Rawahi, N., Tauber W., Han, J., Nas, S., and Jan, Y.J., 2001, "A Front-Tracking Method for the Computations of Multiphase Flow", *Journal of Computational Physics*, **169**, pp.708-759.
- [18] Stone, H.A., 1990, "A Simple Derivation of the Time-Dependent Convective-Diffusion Equation for Surfactant Transport along a Deforming Interface", *Physics of Fluids*, **A2(1)**, pp.111-112.
- [19] Ferziger, J.H., 2003, "Interfacial Transfer in Tryggvason's Method", *International Journal for Numerical Methods in Fluids*, **41**, pp.551-560.